

Predicted energy-loss spectrum of low-dimensional plasmons in a metallic strip monolayer on a semiconductor surface

Takeshi Inaoka

Department of Materials Science and Technology, Faculty of Engineering, Iwate University, 4-3-5 Ueda, Morioka, Iwate 020-8551, Japan

(Received 7 September 2004; revised manuscript received 29 November 2004; published 10 March 2005)

In view of high-resolution electron-energy-loss spectroscopy, we predict the energy-loss spectrum of low-dimensional (LD) plasmons in a metallic strip monolayer on a semiconductor surface. By means of the time-dependent local density approximation, we calculate the dynamical response of our electron system to some typical trajectories of a probe electron incident on the surface along the strip. As shown in our previous work, the energy dispersion of the LD plasmons is composed of a series of dispersion branches where the node number in oscillation of the induced electron density across the strip increases one by one with ascending energy. These branches can produce a series of loss peaks in the spectrum. The branch of the two-node modes gives rise to an outstanding loss peak, and the branches of the zero-node modes (symmetric edge plasmons) and the four-node modes also create significant loss peaks, when the intersection of the scattering plane with the surface plane runs around the center line of the strip region. The branch of the one-node modes (antisymmetric edge plasmons) yields a remarkable loss peak, when the intersection runs just near one of the strip edges. These loss peaks should actually be observed in the spectrum, if there are a sufficient number of strip regions in a surface area illuminated by an electron beam.

DOI: 10.1103/PhysRevB.71.115305

PACS number(s): 73.21.-b, 73.63.-b, 73.22.-f

I. INTRODUCTION

The Si(111)- $\sqrt{3}\times\sqrt{3}$ -Ag surface can be produced by depositing one monolayer of Ag atoms on a Si(111)- 7×7 surface.¹⁻³ This surface has a surface-state band named the S_1 -state band, which provides an ideal two-dimensional (2D) system of conduction electrons.^{4,5} The electron density in the S_1 -state band varies among experiments, because it is significantly affected by a tiny quantity of additional Ag adatoms or other possible dopant impurities or surface states.⁶⁻⁸ By means of high-resolution electron-energy-loss spectroscopy (HREELS), Nagao *et al.* have clearly observed 2D plasmons owing to the S_1 -state band that occur in a virtually infinite area.⁹ Taking account of exchange-correlation effects, Inaoka *et al.* have examined the 2D plasmons in relation to the above HREELS measurements.¹⁰

The conduction electrons due to the S_1 -state band are confined in each $\sqrt{3}\times\sqrt{3}$ -Ag domain surrounded by atomic steps or out-of-phase boundaries, as is observed by low-temperature scanning tunneling microscopy (STM).^{2,11} Near the step or boundary in the STM images appear those standing waves which originate from interference of electronic waves impinging on and reflected from the step or boundary. This clearly indicates the conduction-electron character and the confinement to each $\sqrt{3}\times\sqrt{3}$ -Ag domain. A finite domain of the $\sqrt{3}\times\sqrt{3}$ -Ag structure realizes an ideal 2D conduction-electron system constrained to a finite region which can sustain low-dimensional (LD) plasmons including edge plasmons and area plasmons.

We are concerned with a strip domain of the $\sqrt{3}\times\sqrt{3}$ -Ag structure that is formed on a terrace of a stepped surface. The strip domain is assumed to have a finite width and to extend infinitely. In our previous work, using the time-

dependent local-density approximation (LDA), we have investigated the LD plasmons in the strip region¹² and found a series of plasmon dispersion branches where the node number in oscillation of the induced electron density δn across the strip increases one by one with ascending energy.¹³ The induced electron-density distribution δn of each mode with an even (including zero) node number is *symmetric* with respect to the center line along the strip, while the δn distribution of each mode with an *odd* node number is *antisymmetric* with respect to the center line. The zero-node¹² and one-node¹³ modes are edge plasmons with their δn distribution localized near the edges. The δn distribution of each mode with the node number $j\geq 2$ forms a standing-wave pattern with its free ends at both the edges and with the node number assigned, when the inverse wave number q^{-1} is longer than or comparable to the period of the δn oscillation across the strip. With an increase in q , each inside part of δn in its standing-wave pattern extends wider, and the mode evolves to the area plasmon with approach of the mode energy to that of the 2D plasmons in the infinite area.^{12,13} This evolution occurs in a lower- q range when j is smaller. With further increase in q , the δn distribution ends up with a simple pattern extending monotonously across the strip.¹³

In the present work, we investigate the energy-loss spectrum of the LD plasmons in the strip region in view of the HREELS. By combining the time-dependent LDA calculation of the LD plasmons with the kinematic theory of the HREELS, we calculate the energy-loss probability of the LD plasmons for each of some typical trajectories of a probe electron. The plasmon dispersion branches produce a sequence of energy-loss peaks in the spectrum. Our analysis shows which dispersion branches are most likely to be observed.

II. THEORY

In this section, we describe a theoretical framework for our following analysis. The phrase ‘‘surface plane’’ used here denotes a plane right on a semi-infinite dielectric medium of a dielectric constant ϵ_s . We take the x and y axes in the surface plane and the z axis in the surface-normal direction outward. Our model system is constituted of conduction electrons in the surface plane, a jellium sheet in the surface plane that has a finite width D in the x direction and that extends infinitely in the y direction, and a confining potential $V_C(x)$ due to an atomic step or an out-of-phase boundary. The potential $V_C(x)$ is assumed to be flat inside the jellium strip and to bend up parabolically as $\gamma(x-x_e)^2$ just outside the jellium edge at $x=x_e$. To form a numerical basis for examining electronic excitations, we first calculate the ground state of our electron system.¹³

Next, we consider the dynamical response of our electron system to the external potential U . This response involves the energy loss which is equivalent to the work performed on our electron system by U . The total energy loss due to this response can be expressed as

$$W_T = \frac{1}{\epsilon_t} \int d^2\mathbf{R} \int dt \delta n(\mathbf{R}, t) \frac{\partial}{\partial t} U(\mathbf{R}, t), \quad (1)$$

where \mathbf{R} is a 2D position vector in the surface plane [$\mathbf{R} = (x, y)$], and $\delta n(\mathbf{R}, t)$ and $U(\mathbf{R}, t)$ denote the induced electron density and external potential at position \mathbf{R} and time t , respectively. The dielectric constant ϵ_t defined by $\epsilon_t = (\epsilon_s + 1)/2$ represents the effect of polarization of the semi-infinite dielectric medium. Substitution of the Fourier integrals

$$\delta n(\mathbf{R}, t) = \int \frac{dq}{2\pi} \int \frac{d\omega}{2\pi} \delta n(x, q, \omega) \exp[i(qy - \omega t)] \quad (2)$$

and

$$U(\mathbf{R}, t) = \int \frac{dq}{2\pi} \int \frac{d\omega}{2\pi} U(x, q, \omega) \exp[i(qy - \omega t)] \quad (3)$$

into Eq. (1) yields

$$W_T = \int_0^\infty d\omega \omega P(\omega), \quad (4)$$

where $P(\omega)$ is written as

$$P(\omega) = \frac{1}{\pi\epsilon_t} \int \frac{dq}{2\pi} \int dx |U(x, q, \omega)|^2 \text{Im} \left[-\frac{\delta n(x, q, \omega)}{U(x, q, \omega)} \right]. \quad (5)$$

In Eqs. (2)–(5), the symbols q and ω signify the wave number in the y direction (along the strip) and the angular frequency, respectively. In Eq. (5), the symbol ‘‘Im’’ stands for the imaginary part. As is implied in Eq. (4), the quantity $P(\omega)d\omega$ indicates the probability that there occurs an energy loss between $\hbar\omega$ and $\hbar(\omega+d\omega)$.

In our analysis of the HREELS, the external potential U is produced by a probe electron. In scattering, the probe electron has the Coulomb interaction with induced charges in-

volved in the LD plasmons. In treating this dipole scattering, it is a good approximation to assume that the probe electron follows a classical trajectory.^{14,15} The energy loss $\hbar\omega$ in scattering is small compared with the incident energy E_0 , and scattered directions are sharply concentrated about the specular-reflection direction. Accordingly, we assume an elastic and specular-reflection trajectory. The probability $P(\omega)$ in Eq. (5) obtained in this way represents the energy-loss probability when the probe electron travels along the so-called (00) beam. If the probe electron is incident along the strip and the scattering plane intersects with the surface plane on a line at $x=x_s$, the position of the probe electron is expressed by

$$x(t) = x_s, \quad y(t) = V_y t, \quad \text{and} \quad z(t) = V_z |t|. \quad (6)$$

Here, three constants x_s , $V_y (>0)$, and $V_z (>0)$ signify a position in the x direction, a velocity in the y direction (along the strip), and a velocity in the z direction, respectively. The probe electron following this trajectory generates the external potential

$$U(x, q, \omega) = \frac{2\pi e^2}{A(q, \omega)} \exp \left[-\frac{A(q, \omega)}{V_z} |x - x_s| \right], \quad (7)$$

where $A(q, \omega)$ is defined by

$$A(q, \omega) = \sqrt{(\omega - qV_y)^2 + (qV_z)^2}. \quad (8)$$

By means of the time-dependent LDA, we calculate $\delta n(x, q, \omega)$ due to the response of our electron system to $U(x, q, \omega)$. The calculational scheme is explained in Ref. 13. To obtain the probability of the probe electron undergoing an energy loss $\hbar\omega$ and entering an analyzer window, we perform the q integration in Eq. (5) in a range corresponding to scattering into the analyzer window.

III. RESULTS AND DISCUSSION

By virtue of the theoretical scheme in Sec. II, we investigate the energy-loss spectrum with the LD plasmons for some trajectories of the probe electron. The electron density n_0 in the neutral condition (or the uniform ion density in the jellium strip), the electron effective-mass ratio m^*/m_0 , and the dielectric constant ϵ_s of the semiconductor substrate are taken to be $n_0 = 3.8 \times 10^{13} \text{ cm}^{-2}$, $m^*/m_0 = 0.41$, and $\epsilon_s = 11.5$,¹⁶ respectively. Here, the symbol m_0 signifies the free-electron mass. The above values of n_0 and m^*/m_0 have been determined by fitting the calculated results with the experimental ones in our previous analysis of the 2D plasmons in Ref. 10. The width D of the jellium strip, the parameter γ in $V_C(x)$, and a relaxation-rate constant η in the susceptibility describing the response of our electron system are chosen to be $D = 300 \text{ \AA}$, $\gamma = 20 \text{ meV/\AA}^2$, and $\eta = 2 \text{ meV}$, respectively, as in our previous analysis of the LD plasmons in Refs. 12 and 13. We employ a considerably small value of η so that we can clearly resolve adjacent or fine loss peaks in the energy spectrum. This selection of the η value has no substantial influence on the spectrum as long as its value is small compared with the energy width of each plasmon loss peak in the spectrum, as displayed below in Fig. 3.

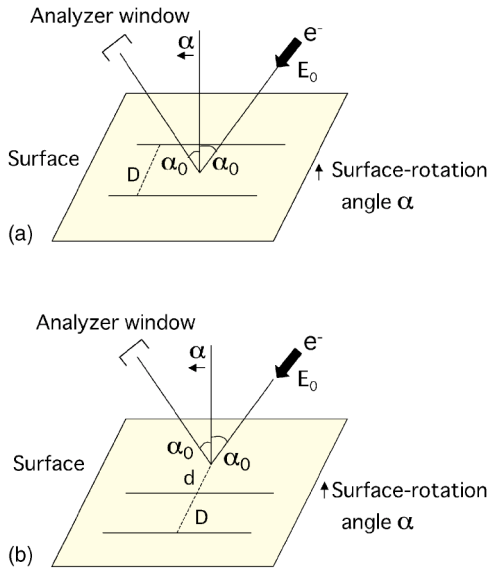


FIG. 1. Scattering geometry of two kinds of trajectories of probe electrons. The intersection of the scattering plane with the surface plane is on the center line of the strip region (a) and at a distance d from the nearer edge of the jellium strip (b). Initially, the analyzer window is adjusted to the specular-reflection direction, as shown in this figure. To shift the probed dispersion region, the surface plane is rotated by an angle α by tilting the surface normal in the scattering plane toward the direction of the analyzer window.

We consider an experimental scheme with the surface plane rotated,⁹ as illustrated in Fig. 1. Initially, we adjust the analyzer window to the specular-reflection direction—namely, to the center of the so-called dipole lobe—as shown in this figure. As we rotate the surface plane gradually, the center of the dipole lobe deviates from the analyzer window increasingly. This shift of the dipole lobe involves that of the probed dispersion region. As stated in Sec. II, we assume that the probe electron is incident in the strip-parallel direction and the scattering plane intersects with the surface plane on a line at $x=x_S$. In panel (a), the line of $x=x_S$ coincides with the center line of the strip region, while, in panel (b), the line runs outside the strip region at a distance d from the nearer edge of the jellium strip. We rotate the surface plane by an angle α by tilting the surface normal in the scattering plane toward the direction of the analyzer window. The incident angle α_0 and the incident energy E_0 are taken to be $\alpha_0=6^\circ$ and $E_0=12.4$ eV, respectively, as in the HREELS experiment of Ref. 9. The angle α_0 is measured from the surface normal of the initial surface plane before rotation. The analyzer window is assumed to be circular with half angle θ_a . We employ the value of $\theta_a=0.58^\circ$ determined by fitting the calculated energy-loss probability owing to the 2D plasmons to the experimental one.¹⁰

Figure 2 shows the energy dispersion of the LD plasmons in the strip region.¹³ The dashed curve marked “2DPL” and starting from the origin represents the dispersion of the 2D plasmons in the infinite area.¹⁰ This dispersion can be obtained by using a local-field-correction theory that takes account of the exchange-correlation effects.^{17,18} The single-particle excitation (SPE) continuum for the infinite area

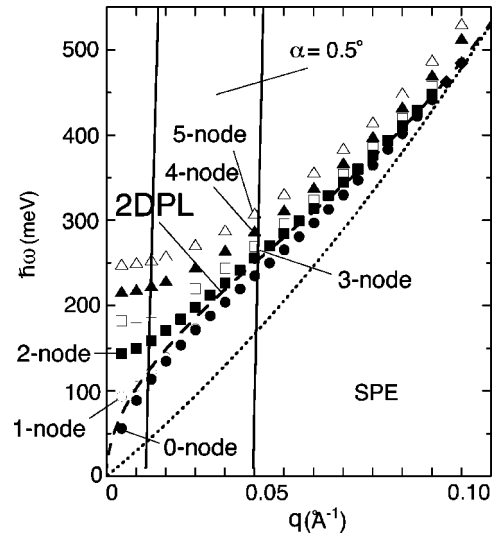


FIG. 2. Energy dispersion of low-dimensional plasmons in a two-dimensional electron system confined in a strip region. The electron density, the electron effective-mass ratio, and the width of the jellium strip are taken to be $n_0=3.8 \times 10^{13}$ cm⁻², $m^*/m_0=0.41$, and $D=300$ Å, respectively. A series of points marked “ j -node” indicates the dispersion branch of the j -node modes. The dashed curve shows the energy dispersion of two-dimensional plasmons (2DPL’s) in an infinite area. The single-particle excitation (SPE) continuum for the infinite area extends on the right side of the dotted curve. A region between two vertical lines exhibits the whole probed dispersion region for $\alpha=0.5^\circ$ that involves all the scattering into the analyzer window. The kinematic-parameter values are specified in Fig. 3.

extends on the right side of the dotted curve. A region between two vertical lines indicates the whole probed dispersion region for $\alpha=0.5^\circ$ that covers all the scattering into the analyzer window with $\theta_a=0.58^\circ$. As stated in Sec. I, the dispersion of the LD plasmons is composed of a series of dispersion branches where the node number increases one by one with ascending energy.¹³ Each dispersion branch with node number $j(=0,1,2,\dots)$ is marked “ j -node.” The one-node branch accords virtually with the zero-node branch except in a small- q region of $q \leq 0.02$ Å⁻¹.

Figure 3 exhibits the ω dependence of the energy-loss probability $P(\omega)$ for some trajectories of the probe electron in Fig. 1. In panel (a), the intersection of the scattering plane with the surface plane agrees with the center line along the strip [see Fig. 1(a)]. In panel (b), the intersection runs at a distance $d=20, 50,$ and 100 Å from the nearer edge of the jellium strip [see Fig. 1(b)]. A series of loss peaks in each spectrum originates from a sequence of dispersion branches passing through the probed dispersion region [see Fig. 2]. When the scattering plane intersects with the surface plane on the center line, the external potential U at the surface becomes symmetric with respect to the center line, and it excites only the symmetric plasmon modes with even (including zero) mode numbers. Accordingly, the loss peaks in Fig. 3(a) can be ascribed to the zero-node, two-node, four-node, and six-node branches, respectively, in order of increasing energy. The zero-node modes are the symmetric edge plasmons. In each of the two-node, four-node, and six-

node modes, the δn oscillation across the strip region has its loop on the center line of the strip.¹³ The probe electron incident on the center line interacts most strongly with those two-node modes where their central part in the δn distribution is extending most widely just below the trajectory, and in addition, which are already beginning to acquire the character of the area plasmon in the probed q range. Consequently, the two-node branch yields a loss peak of outstanding intensity. The zero-node and four-node branches also create significant loss peaks.

When the intersection of the scattering plane with the surface plane runs outside the strip region, the external potential U at the surface involves an antisymmetric component as well as a symmetric one. This potential excites both the symmetric modes with even node numbers and the antisymmetric modes with odd node numbers. Therefore, every dispersion branch produces a loss peak or a shoulder in the spectrum [see Fig. 3(b)]. The major loss peak in the spectrum arises mainly from the one-node branch, and the zero-node branch brings about a shoulder on the lower-energy side of the major loss peak. The dispersion branches with node numbers $j \geq 2$ lead to a series of loss peaks superimposed on the higher-energy side of the above major loss peak. The probe electron passing near one edge interacts quite strongly with the one-node modes: namely, the *antisymmetric edge* plasmons. The strong interaction with the antisymmetric plasmons originates from the fact that the probe electron induces transverse movements of conduction electrons, leading to an antisymmetric δn distribution.

With an increase in d , the spectrum intensity declines quickly without any substantial change in the spectrum structure. This quick intensity decline can be attributed to an exponential factor in Eq. (7). As the scattering plane becomes separated farther from the strip edge, the (q, ω) component of U at any position of x in the strip region attenuates exponentially, which results in the quick intensity decline.

Here, we turn our attention to the 2D plasmons in an infinite or virtually infinite area. By means of the HREELS, the 2D plasmons have clearly been observed in a broad q region, until the plasmon mode enters the single-particle excitation continuum and decays immediately.⁹ This implies that the 2D plasmons maintain sufficient energy-loss intensity in the broad q range. Using the theoretical scheme in Ref. 10, we can calculate the energy-loss probability $P(\omega)$ corresponding to this experiment. This analysis shows that we can definitely observe the 2D plasmon whose resonance intensity in $P(\omega)$ is on the order of 10^{-5} .

In view of the intensity scale on the ordinate in Fig. 3, several main loss peaks due to the LD plasmons in these spectra are considered to have observable intensity. Here, we should recall that an incident electron beam in the HREELS has a finite transverse section whose size is large compared with the strip width and that scattering of this electron beam involves various trajectories of probe electrons. From Figs. 3(a) and 3(b), we can expect to observe the loss peak owing to the two-node branch, the one due to the one-node branch (antisymmetric edge plasmons), and a few ones of the other symmetric-mode branches, such as the zero-node branch (symmetric edge plasmons) and the four-node branch. To actually observe these loss peaks expected, we probably need

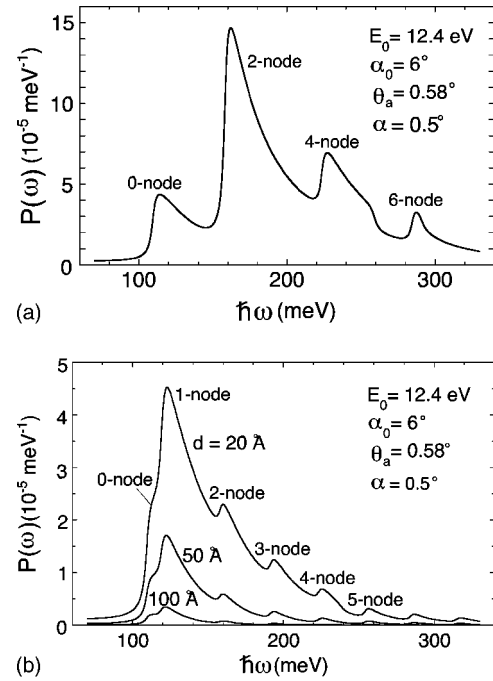


FIG. 3. ω dependence of the energy-loss probability of the low-dimensional plasmons in the strip region for some trajectories of a probe electron. The spectra in (a) and (b) correspond to the trajectories in (a) and (b) of Fig. 1, respectively. In the spectrum (b), the distance d is taken to be $d=20, 50,$ and 100 \AA . Each loss peak marked “ j -node” originates from the dispersion branch of the j -node modes. The incident energy and the incident angle of the probe electron, the rotated angle of the surface plane, and the half angle of the circular analyzer window are taken to be $E_0=12.4 \text{ eV}$, $\alpha_0=6^\circ$, $\alpha=0.5^\circ$, and $\theta_a=0.58^\circ$, respectively. The angle α_0 is measured from the surface normal of the initial surface plane before rotation.

to make a parallel array of strip regions that occupy a considerable fraction of the surface area illuminated by the electron beam.

Here, we make a brief comment on the strip-width dependence on the LD plasmons. With a decrease in the width, each j -node branch with $j \geq 1$ shifts upward remarkably, and the energy separation between neighboring branches becomes larger.¹⁹ This width dependence of the dispersion branches should give rise to the peak shift in the energy-loss spectrum.

When strip regions are arranged at short intervals, the LD plasmons in one region interact with those in another near region, particularly in a small- q range. It is our future problem to examine how this interaction operates in these coupled LD plasmons. Our analysis of the LD plasmons in a single-strip region forms a basis for solving this future problem.

IV. SUMMARY

Bearing the HREELS in mind, we have investigated the energy-loss spectrum of the LD plasmons in the strip region

for some trajectories of a probe electron. A series of dispersion branches of the LD plasmons can create a sequence of loss peaks in the spectrum. Particularly, the dispersion branch of the two-node modes and that of the one-node modes (antisymmetric edge plasmons) cause loss peaks of outstanding intensity. A few dispersion branches of the other symmetric modes, such as the zero-node modes (symmetric edge plasmons) and the four-node modes, also give rise to loss peaks of considerable intensity. These specific dispersion branches should be observed in the spectrum if there are

a sufficient number of strip regions in a surface area illuminated by an incident electron beam.

ACKNOWLEDGMENTS

This work is supported by a Grant-in-Aid for Scientific Research from the Ministry of Education, Science, Sport, and Culture under Grant No. 13640315. Numerical calculations in the present work were performed at the Information Synergy Center of Tohoku University and the Iwate University Super Computing and Information Sciences Center.

-
- ¹S. Hasegawa, X. Tong, S. Takeda, N. Sato, and T. Nagao, *Prog. Surf. Sci.* **60**, 89 (1999).
- ²S. Hasegawa, N. Sato, I. Shiraki, C. L. Petersen, P. Bøggild, T. M. Hansen, T. Nagao, and F. Grey, *Jpn. J. Appl. Phys., Part 1* **39**, 3815 (2000).
- ³S. Hasegawa and F. Grey, *Surf. Sci.* **500**, 84 (2002).
- ⁴S. Hasegawa, X. Tong, C.-S. Jiang, Y. Nakajima, and T. Nagao, *Surf. Sci.* **386**, 322 (1997).
- ⁵X. Tong, C.-S. Jiang, and S. Hasegawa, *Phys. Rev. B* **57**, 9015 (1998).
- ⁶Y. Nakajima, S. Takeda, T. Nagao, S. Hasegawa, and X. Tong, *Phys. Rev. B* **56**, 6782 (1997).
- ⁷R. I. G. Uhrberg, H. M. Zhang, T. Balasubramanian, E. Landemark, and H. W. Yeom, *Phys. Rev. B* **65**, 081305 (2002).
- ⁸J. N. Crain, K. N. Altmann, C. Bromberger, and F. J. Himpsel, *Phys. Rev. B* **66**, 205302 (2002).
- ⁹T. Nagao, T. Hildebrandt, M. Henzler, and S. Hasegawa, *Phys. Rev. Lett.* **86**, 5747 (2001).
- ¹⁰T. Inaoka, T. Nagao, S. Hasegawa, T. Hildebrandt, and M. Henzler, *Phys. Rev. B* **66**, 245320 (2002).
- ¹¹N. Sato, S. Takeda, T. Nagao, and S. Hasegawa, *Phys. Rev. B* **59**, 2035 (1999).
- ¹²T. Inaoka, *Phys. Rev. B* **68**, 041301 (2003).
- ¹³T. Inaoka, *J. Phys. Soc. Jpn.* **73**, 2201 (2004).
- ¹⁴W. L. Schaich, *Phys. Rev. B* **24**, 686 (1981).
- ¹⁵Ph. Lambin, A. A. Lucas, and J. P. Vigneron, *Surf. Sci.* **182**, 567 (1987).
- ¹⁶H. R. Philipp and H. Ehrenreich, *Phys. Rev.* **129**, 1550 (1963).
- ¹⁷K. S. Singwi, M. P. Tosi, R. H. Land, and A. Sjölander, *Phys. Rev. Lett.* **176**, 589 (1968).
- ¹⁸M. Jonson, *J. Phys. C* **9**, 3055 (1976).
- ¹⁹T. Inaoka (unpublished).